B_{80} and Other Medium-Sized Boron Clusters: Core−Shell Structures, Not Hollow Cages

Jijun Zhao,*,† Lu Wang,† Fengyu Li,†,‡ and Zhongfang Chen*,‡

Key Laboratory of Materials Modification by Laser, Ion and Electron Beams (Dalian University of Technology), Ministry of Education, Dalian 116024, China, College of Advanced Science and Technology, Dalian University of Technology, Dalian 116024, China, and Department of Chemistry, Institute of Functional Nanomaterials, University of Puerto Rico, San Juan, PR 00931

Received: March 2, 2010; Revised Manuscript Received: July 3, 2010

Unbiased search on the potential energy surface of medium-sized boron clusters, with B_{80}, B_{74}, and B_{68} as representatives, was carried out using simulated annealing incorporated with first-principles molecular dynamics. These boron clusters thermodynamically prefer the B_{12}-centered core−shell structures, which resemble the fragment of bulk boron solids. Though these core−shell clusters lack a descriptive symmetry and may not be the true global minima, the core−shell B_{80} is about 25 meV/atom lower in energy than the widely assumed highly stable "magic" B_{80} fullerene. The electronic states and photoelectron spectra of these clusters are closely correlated to the structural motif, which may be helpful for detecting the cluster configurations in experiments.

1. Introduction

Boron is the fifth element in the periodic table and the first one to possess a p electron. The unique characters of boron, such as short covalent radius, electron deficiency, and flexibility to adopt sp^2 hybridization and three-center bonds, endow boron clusters probably the most intriguing chemical bonding, which continues to surprise us. Many breakthroughs have been achieved in the past decade. For example, pure boron clusters are established to be planar or quasi-planar up to 19 atoms,[1,2] and the planar-to-tubular structural transition occurs at B_{20} which has a double-ring-tubular (DRT) configuration.[3]

One recent superstar of boron clusters is B_{80} (Figure 1a), a fullerene-like hollow cage proposed by Szwacki et al.[4] This aesthetically pleasant molecule quickly triggered a hot wave of designing B_{80}-based nanomaterials, for example, endohedral complexes,[5] solids,[6] and hydrogen storage materials.[7] Moreover, inspired by B_{80} with optimal balance of two-center and three-center bonds, new construction rules for stable boron fullerenes were proposed, and a large boron fullerene family including some new members with even higher stability than B_{80}, was predicted.[8,9] More importantly, the chemical bonding of B_{80} fullerene with triangular and hexagonal motifs led scientists to reexamine the conventionally assumed structures of boron sheets and nanotubes consisting of only puckered triangular motifs: the more stable α boron sheet[10] was proposed, the more favorable boron nanotubes[10,11] were designed, and the boron nanoribbons[12] were constructed using the α-sheet as the precursor. In short, the novel chemical structure and bonding of B_{80} is so important that it has brought brand new insights into the essences of boron nanomaterials science.

Currently, the B_{80} hollow fullerene is generally believed to be most stable among the 80-atom boron clusters;[4,9,13] however, its relative stability with regard to the other possible structural patterns has not been established. The same is also true for many other medium-sized boron clusters.[8,9] In this paper, we performed unbiased search on the potential energy surface of medium-sized boron clusters, with B_{80}, B_{74}, and B_{68} as representatives, using simulated annealing (SA) incorporated with first-principles molecular dynamics (FPMD) and revealed that these clusters prefer B_{12}-centered core−shell structures energetically, for example, the core−shell B_{80} cluster prevails for the "magic" B_{80} cage by about 25 meV/atom. These core−shell boron clusters resemble the structural and electronic properties of β-boron solid and constitute a pathway from microclusters to macroscopic solids.

2. Computational Methods

Our unbiased search on the potential energy surface of B_{80}, B_{74}, and B_{68} clusters was carried out using simulated annealing incorporated with first-principles molecular dynamics. The initial configuration was generated from scratch (i.e., totally by random) and annealed from 3000 to 400 K stepwise by 50 K increment. At each temperature, FPMD simulation in the *NVT* ensemble lasted for 10 ps with a time step of 0.5 fs. The FPMD simulations employed a planewave basis (257 eV cutoff energy) and ultrasoft pseudopotentials, as implemented in the VASP program.[14] The exchange−correlation interaction was described

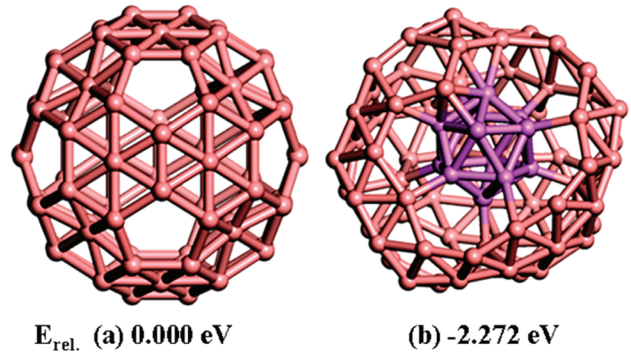

Figure 1. Optimized structures of (a) the B_{80} fullerene hollow cage[4] and (b) the B_{80} core−shell cluster from first-principles simulated annealing. The interior B_{12} icosahedron in the core−shell clusters are highlighted in purple.

* Corresponding authors. E-mail:zhaojj@dlut.edu.cn (J.Z.); zhongfangchen@gmail.com (Z.C.).
† Dalian University of Technology.
‡ University of Puerto Rico.

10.1021/jp1018873 © 2010 American Chemical Society
Published on Web 08/10/2010

by the Perdew–Burke–Enzerhof (PBE) functional within the generalized gradient approximation (GGA). The cluster was placed in a sufficiently large supercell (18 Å) to avoid interactions with its periodic images.

The cluster configurations from FPMD-SA search were further optimized using the all-electron DMol^3 program[15] with a double numerical basis set including *d* polarization (DND) and the PBE functional. Vibrational analyses were performed to ensure that the optimized structures are the true minima on the potential energy surface. The same PBE/DND scheme has been used in a recent study of B_n clusters ($n = 60-106$).[9] At the PBE/DND level of theory, the lattice constant and cohesive energy for rhombohedra β-boron solid are $a = 10.125$ Å and $E_c = 6.219$ eV/atom, respectively, which agree reasonably well with the experimental values of $a = 10.17$ Å[16] and $E_c = 5.81$ eV/atom.[17] In this paper, all the energy and structural parameter analyses were based on the PBE/DND simulations, unless stated otherwise.

Nucleus-independent chemical shifts (NICS, in ppm),[18] a simple and efficient method to evaluate aromaticity, were computed at the cage or ring centers of the PBE/DND optimized B_{80} cluster geometries using the gauge-independent atomic orbital (GIAO) method at the B3LYP/6-31G* level of theory employing the Gaussian 03 program.[19]

3. Results and Discussion

The unbiased FPMD-SA search resulted in an amorphous core–shell B_{80} cluster (Figure 1b and Table S2 in the Supporting Information), in which the center is an icosahedral B_{12}, the dominant unit in the crystalline and amorphous boron solids.[16,20] Note that this core–shell structure is not complete since the remaining 68 boron atoms in the outer shell are insufficient to fully cover the B_{12} core. Part of the B_{12} core links with the cap atoms on the pentagonal pyramidal B_6 or hexagonal pyramidal B_7 units from the outer shell, satisfying the "Aufbau principles" (according to which the highly stable boron species are composed of either hexagonal or pentagonal fundamental units);[21] other core atoms on B_{12} are either naked or connected with the edge atoms of the incomplete outer shell (see the Supporting Information). The outer shell mainly comprises triangular facets as a consequence of the three-center bonds.[22] To balance the excess electrons from the triangles,[10] on the outer surface there are several pentagonal, hexagonal, and heptagonal holes, and several double rings intercrossing with each other, similar to the α boron sheet and other hollow boron cages.[8–10]

Most importantly, the "magic" fullerene cage of B_{80} (Figure 1a) is less stable than the present core–shell structure from FPMD-SA search (Figure 1b) by 28.4 meV/atom at the PBE/DND level of theory (21.7 meV/atom at PBE with plane planewave basis and ultrasoft pseudopotentials using VASP code, 22.6 and 16.8 meV/atom, respectively, at PBE/6-31G* and B3LYP/6-31G* using Gaussian 03 program; see Table S1 in the Supporting Information). This finding is in line with Li et al.'s most recent finding that the asymmetric isomer is ~20 meV/atom lower in energy than the boron buckyball B_{80}.[23] However, Li et al's B_{80} has a fully covered B_{12} core, while ours has a partially covered B_{12} core-shell structure, and is 1.04 eV lower in energy at the B3LYP/6-31G* level of theory (see Figure S5 in the Supporting Information).

The energetic preference of core–shell structure can be related to the fact that there is no graphene-like planar structure for any allotropes of the boron solids.[16,20] Even though the B_{80} cage is isoelectronic to C_{60} and exhibits remarkable stability,[9,13,24] it has no bulk counterpart in the solid phases, unlike C_{60} and graphite. On the contrary, the present core–shell structures built by the B_{12} core plus the B_6/B_7 pyramidal units can be viewed as pieces of boron solids. The electron-deficient nature of boron leads to a high coordination number (CN) for each boron atom, for example, CN = 6 for α-boron solid and CN = 6.4 for β-solid. The coordination number of the present core–shell B_{80} cluster is 5.45, higher than that of the B_{80} fullerene (CN = 5.25). Similar to the present situation, Si_{60}, as for the isoelectronic system of C_{60}, also prefers a core–shell structure instead of the hollow buckyball cage.[25]

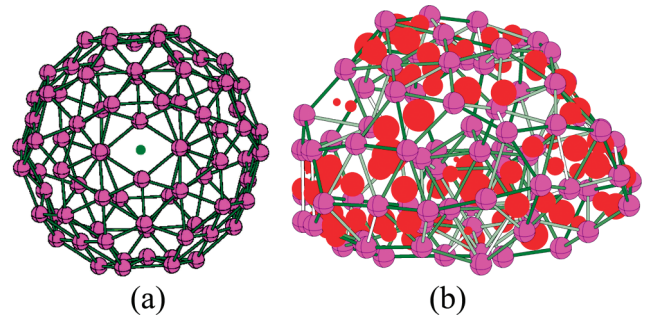

Figure 2. Plots of total NICS contributions (a) at the cage center of B_{80} (T_h) and (b) at the cage and ring centers of the core–shell B_{80} cluster. The green and red dots denote paratropic (antiaromatic) and diatropic (aromatic) ring currents, respectively.

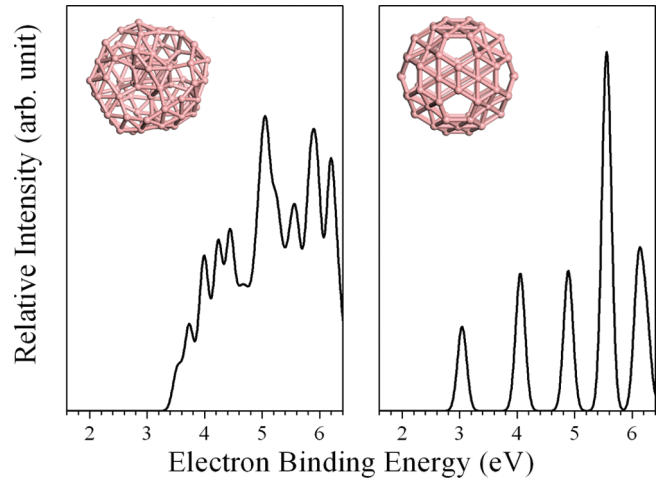

Figure 3. Simulated photoelectron spectrum of the B_{80}^- cluster with core–shell (left) and fullerene cage structures (right).

The lower stability of the B_{80} fullerene cage may be attributed to its weak antiaromaticity,[26] as indicated by its positive nucleus-independent chemical shift (NICS)[18] value (14.9 ppm) at the cage center. In contrast, the core–shell B_{80} cluster is highly aromatic, the NICS value at the B_{12} core center is −26.5 ppm, and those at the ring centers are in the range of −42.4 to −0.10 ppm (Figure 2). The aromaticity and the partially closed packing are the two major factors for the higher stability of the core–shell B_{80} cluster than the B_{80} hollow cage, which follows the general principles Chen et al. proposed to achieve stable spherical clusters.[27]

The correlation between the atomic structure and electronic states makes the photoelectron spectroscopy an efficient way to identify the most favorable configurations of smaller B_n clusters ($n \leq 20$).[1–3] The simulated photoelectron spectra (PES) for the core–shell and fullerene cage isomers of B_{80}^- are shown in Figure 3. The vertical detachment energy (VDE) corresponding to the first peak on PES is 3.529 eV for the core–shell isomer and 3.041 eV for the hollow cage. With a small

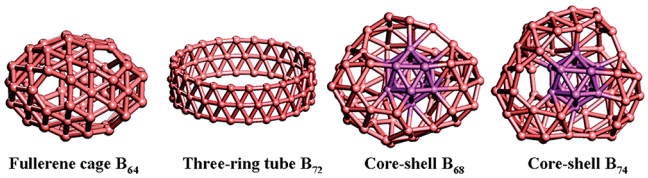

Figure 4. Optimized structures for B_n clusters (n = 64−80) of representative structural motifs.

HOMO−LUMO gap (0.347 eV) for the neutral cluster, the first (X-band) and second (A-band) peaks of PES for the core−shell B_{80}^- are rather close. In contrast, there is a 1 eV separation between the X and A bands for the B_{80}^- fullerene. The distinct differences in the PES features and VDE values will help differentiate these isomers experimentally. However, distinguishing the spectra in reality will be very difficult. Not only these two isomers will be present, but also other 80-sized isomer clusters and other sized boron clusters may also exist in the cluster beam, making overall spectral analysis hard.

We analyzed the vibrational density of states and IR spectra of the cage and core−shell structures of the B_{80} cluster from PBE/DND calculations (see Figures S2 and S3 in the Supporting Information). Clearly the core−shell B_{80} cluster exhibits more high-energy frequencies.

To assess the relative stabilities of the these two B_{80} isomers at high temperature, we computed their vibrational free energies and total free energies. The vibrational free energy (with inclusion of zero-point energy) of the hollow B_{80} cluster is lower than that of the core−shell B_{80} cluster by 8.4 meV/atom at room temperature (298 K); however, this can only compensate one-third of the energy difference of these two isomers at 0 K (about 28 meV/atom). When the total free energies are considered, though the B_{80} cage has a larger entropy at higher temperatures, the core−shell structure of B_{80} is still more favorable by 9.5 meV/atom than the cage structure at 1000 K (see Figure S4 in the Supporting Information). Thus, the core−shell B_{80} will dominate even at high temperatures.

Encouraged by the above results and the recent finding that B_{84}[28] and B_{98}−B_{102}[9] also prefer core−shell clusters, we extended our FPMD-SA search to smaller clusters and found that B_{68} and B_{74} also prefer the B_{12}-centered core−shell structures, and they are lower in energy than the hollow cage and tubular configurations (Figure 4).

To understand the growth behavior of the boron clusters, we have considered three structural motifs, namely, the three-ring tubular (TRT) structures for B_{3m} (m = 22, 24, 26),[29] the hollow fullerene cages for B_{64}[8b] and B_{80},[4] and the core−shell structures for B_{68}, B_{74}, and B_{80} from the present simulated annealing incorporated with first-principles molecular dynamics. The typical optimized structures and their size-dependent binding energies of these three motifs are presented in Figures 4 and 5, respectively. Within the size range studied, the core−shell structures always prevail for the hollow cages and the TRT forms, with an energy difference of ca. 30 meV/atom. A double-ring tubular structure was also considered for B_{80}, but it is less stable than the core−shell B_{80} cluster by 134.6 meV/atom. A linear extrapolation of our theoretical binding energies for the core−shell B_{68}, B_{74}, and B_{80} clusters leads to a binding energy of 5.726 eV/atom at B_{101}, which is very close to the binding energy of 5.711 eV/atom computed for the best core−shell cluster of B_{101} (C_s symmetry) reported in ref 9 using the present PBE/DNP scheme.

The above B_{12}-centered core−shell clusters can be viewed as an embryo of the solid phases, as indicated by the high

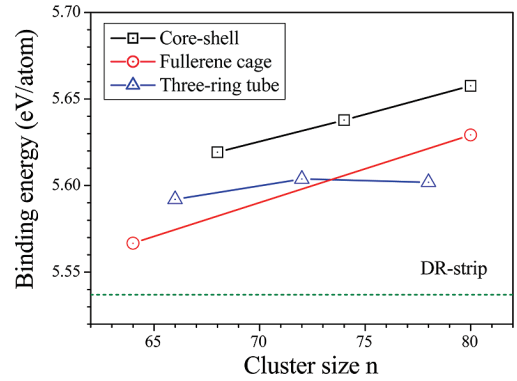

Figure 5. Binding energies for B_n clusters (n = 64−80) of different structural motifs: (squares) core−shell; (triangles) three-ring tubular; (circles) fullerene cages. The dashed line is for the infinite double-ring (DR) strip.

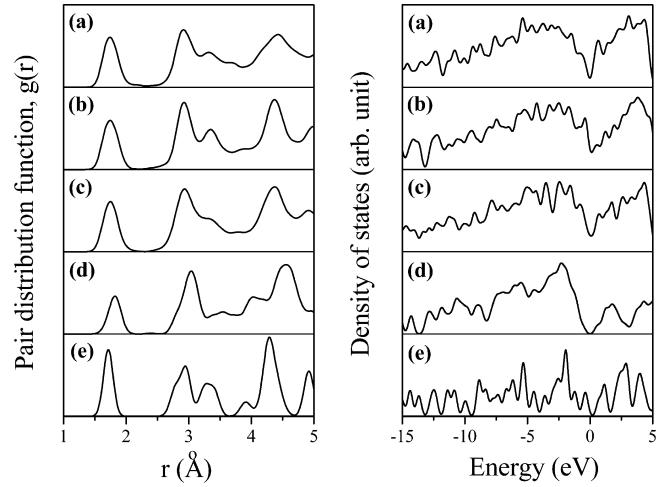

Figure 6. Pair distribution functions (left) and electron density of states (right) for (a) B_{68}, (b) B_{74}, (c) B_{80} core−shell clusters, (d) β-rhombohedral boron solid, and (e) B_{80} hollow cage. The Fermi level is set to zero, and a Gaussian broadening of 0.2 eV was used.

similarities of their pair distribution functions (PDF) and electron density of states (DOS) between these core−shell clusters with those of the β-rhombohedral boron solid (Figure 6). For example, the B_{80} cluster exhibits three major PDF peaks (1.74, 2.92, and 4.37 Å) very close to those in the β-boron (1.80, 3.03, and 4.56 Å), and the amorphous boron solid (1.83, 3.05, and 4.60 Å).[20] The overall feature for the electronic state of these core−shell clusters also resembles well that of the β-rhombohedral solid, in particular, in the vicinity of Fermi level. On the contrary, the PDF and DOS of the hollow B_{80} cage show distinctly different characteristics with regard to the core−shell clusters and β-boron solid.

4. Conclusion

To summarize, unbiased search with first-principles methods revealed the formation of the core−shell structure of the B_{80} cluster, in which a B_{12} icosahedron is partially surrounded by pentagonal or hexagonal pyramidal units of B_6 and B_7, satisfying the "Aufbau principles". This B_{12}-centered core−shell B_{80} cluster energetically prevails the previously assumed "magic" B_{80} cage, and experimental photoelectron spectroscopy can be used to distinguish the configurations of the B_{80} cluster. Similar core−shell structures are also preferred by smaller B_{68} and B_{74} boron clusters. Since the potential energy surfaces of these sized clusters are extremely complicated, we cannot guarantee that

the present lowest-energy structures are the true global minima. However, the general trend about the energetic preference of core−shell structures over fullerene cages should be valid. The present findings not only enrich our knowledge on the structural and electronic properties as well as chemical bonding of boron clusters but also shed some light on the formation of crystalline and amorphous boron solids.

Acknowledgment. This work was supported in China by the NCET-060281 and in the U.S.A. by NSF Grant CHE-0716718, the Institute for Functional Nanomaterials (NSF Grant 0701525), the U.S. Environmental Protection Agency (EPA Grant No. RD-83385601), and in part the National Science Foundation through TeraGrid resources. Z.C. also thanks the 2010 HBCU/MEI Summer Faculty Program to support his stay at Oak Ridge National Lab during which this project was finalized.

Supporting Information Available: The full citation of ref 19, the structure of B_{80} cluster with B_{12} core and incomplete B_{68} outer shell, vibrational density of states and IR spectra of B_{80} with hollow cage and core shell structures, the energy difference between hollow cage and core shell isomers of B_{80}, and Cartesian coordinates for the B_{80} core−shell configuration. This material is available free of charge via the Internet at http://pubs.acs.org.

References and Notes

(1) For most recent reviews, see (a) Alexandrova, A. N.; Boldyrev, A. I.; Zhai, H. J.; Wang, L. S. *Coord. Chem. Rev.* **2006**, *250*, 2811. (b) Zubarev, D. Y.; Boldyrev, A. I. *J. Comput. Chem.* **2008**, *28*, 251.

(2) Huang, W.; Sergeeva, A. P.; Zhai, H. J.; Averkiev, B. B.; Wang, L. S.; Boldyrev, A. I. *Nat. Chem.*, DOI: 10.1038/nchem.534.

(3) Kiran, B.; Bulusu, S.; Zhai, H. J.; Yoo, S.; Zeng, X. C.; Wang, L. S. *Proc. Natl. Acad. Sci. U.S.A.* **2005**, *102*, 961.

(4) (a) Szwacki, N. G.; Sadrzadeh, A.; Yakobson, B. I. *Phys. Rev. Lett.* **2007**, *98*, 166804. (b) Szwacki, N. G.; Sadrzadeh, A.; Yakobson, B. I. *Phys. Rev. Lett.* **2008**, *100*, 159901.

(5) (a) Jin, P.; Hao, C.; Gao, Z. X.; Zhang, S. B.; Chen, Z. *J. Phys. Chem. A* **2009**, *113*, 11613. (b) Li, J. L.; Yang, G. W. *Appl. Phys. Lett.* **2009**, *95*, 133115. (c) Wang, J. T.; Chen, C.; Wang, E. G.; Wang, D. S.; Mizuseki, H.; Kawazoe, Y. *Appl. Phys. Lett.* **2009**, *94*, 133102.

(6) (a) Yan, Q. B.; Zheng, Q. R.; Su, G. *Phys. Rev. B* **2008**, *77*, 224106. (b) Liu, A. Y.; Zope, R. R.; Pederson, M. R. *Phys. Rev. B* **2008**, *78*, 155422. (c) Yan, Q. B.; Zheng, Q. R.; Su, G. *Phys. Rev. B* **2009**, *80*, 104111.

(7) (a) Zhao, Y. F.; Lusk, M. T.; Dillon, A. C.; Heben, M. J.; Zhang, S. B. *Nano Lett.* **2008**, *8*, 157. (b) Wu, G. F.; Wang, J. L.; Zhang, X. Y.; Zhu, L. Y. *J. Phys. Chem. C* **2009**, *113*, 7052. (c) Li, M.; Li, Y. F.; Zhou, Z.; Shen, P.; Chen, Z. F. *Nano Lett.* **2009**, *9*, 1944.

(8) (a) Szwacki, N. G. *Nanoscale Res. Lett.* **2008**, *3*, 49. (b) Yan, Q.; Sheng, X.; Zheng, Q.; Zhang, Li.; Su, G. *Phys. Rev. B* **2008**, *78*, 201401. (c) Zope, R. R.; Baruah, T.; Lau, K. C.; Liu, A. Y.; Pederson, M. R; Dunlap, B. I. *Phys. Rev. B* **2009**, *79*, 161403. (d) Sheng, X. L.; Yan, Q. B.; Zheng, Q. R.; Su, G. *Phys. Chem. Chem. Phys.* **2009**, *11*, 9696. (e) Zope, R. R. *Eurphys. Lett.* **2009**, *85*, 68005. (f) Mukhopadhyay, S.; He, H.; Pandey, R.; Yap, Y. K.; Boustani, I. *J. Phys.: Conf. Ser.* **2009**, *176*, 012028. (g) Özdoan, C.; Mukhopadhyay, S.; Hayami, W.; Güvenç, Z. B.; Pandey, R.; Boustani, L. *J. Phys. Chem. C* **2010**, *114*, 4362.

(9) Prasad, D. L. V. K.; Jemmis, E. D. *Phys. Rev. Lett.* **2008**, *100*, 165504.

(10) (a) Tang, H.; Ismail-Beigi, S. *Phys. Rev. Lett.* **2007**, *99*, 115501. (b) Yang, X. B.; Ding, Y.; Ni, J. *Phys. Rev. B* **2008**, *77*, 041402(R).

(11) Singh, A. K.; Sadrzadeh, A.; Yakobson, B. I. *Nano Lett.* **2008**, *8*, 1314.

(12) Ding, Y.; Yang, X.; Ni, J. *Appl. Phys. Lett.* **2008**, *93*, 043107.

(13) (a) Sadrzadeh, A.; Pupysheva, O. V.; Singh, A. K.; Yakobson, B. I. *J. Phys. Chem. A* **2008**, *112*, 13679. (b) Mukhopadhyay, S.; He, H.; Pandey, R.; Yap, Y. K.; Boustani, I. *J. Phys.: Conf. Series* **2009**, *176*, 012028.

(14) Kresse, G.; Hafner, J. *Phys. Rev. B* **1993**, *47*, 558; **1994**, *49*, 14251.

(15) Delley, B. *J. Chem. Phys.* **1990**, *92*, 508; **2000**, *113*, 7756.

(16) Donohue, J. *The Structures of The Elements*; Wiley: New York, 1974.

(17) Kittle, C. *Introduction to Solid State Physics*, 7th ed.; Wiley: New York, 1996.

(18) (a) Schleyer, P. v. R.; Maerker, C.; Dransfeld, A.; Jiao, H.; Hommes, N. v. E. *J. Am. Chem. Soc.* **1996**, *118*, 6317. (b) Chen, Z.; Wannere, C. S.; Corminboeuf, C.; Puchta, R.; Schleyer, P. v. R. *Chem. Rev.* **2005**, *105*, 3842.

(19) Frisch, M. J.; et al. *Gaussian 03*.

(20) Delaplane, R. G.; Lundström, T.; Dahlborg, U.; Howells, W. S. *AIP Conf. Proc.* **1991**, *231*, 241. (b) Donohue, J. *The Structures of The Elements*; Wiley: New York, 1974.

(21) Boustani, I. *Phys. Rev. B* **1997**, *55*, 16426.

(22) Fujimori, M.; Nakata, T.; Nakayama, T.; Nishibori, E.; Kimura, K.; Takata, M.; Sakata, M. *Phys. Rev. Lett.* **1999**, *82*, 4452.

(23) Li, H.; Shao, N.; Shang, B.; Yuan, L. F.; Yang, J.; Zeng, X. C. *Chem. Commun.* **2010**, *46*, 3878.

(24) Ceulemans, A.; Muya, J. T.; Gopakumar, G.; Nguyen, M. T. *Chem. Phys. Lett.* **2008**, *461*, 226–228.

(25) Zhao, J. J.; Ma, L.; Wen, B. *J. Phys.: Condens. Matter* **2007**, *19*, 226208.

(26) For recent thematic issues on aromaticity, see: (a) *Chem. Rev* **2001**, *101*, May. (b) *Chem. Rev.* **2005**, *105*, October.

(27) Chen, Z.; Neukermans, S.; Wang, X.; Janssens, E.; Zhou, Z.; Silverans, R. E.; King, R. B.; Schleyer, P. v. R.; Lievens, P. *J. Am. Chem. Soc.* **2006**, *128*, 12829–12834.

(28) Shang, B.; Yuan, L. F.; Zeng, X. C.; Yang, J. *J. Phys. Chem. A* **2010**, *114*, 2245–2249.

(29) Tian, F. Y.; Wang, Y. X. *J. Chem. Phys.* **2008**, *129*, 024903.

JP1018873